Condensation of two-dimensional harmonically confined bosons with Bessel-type interactions

A. I. Mese,[1] P. Capuzzi,[2,3,*] S. Aktas,[1] Z. Akdeniz,[4] and S. E. Okan[1]
[1]*Department of Physics, Trakya University, 22030 Edirne, Turkey*
[2]*Instituto de Física de Buenos Aires, Consejo Nacional de Investigaciones Científicas y Técnicas, Argentina*
[3]*Departamento de Física, FCEyN, Universidad de Buenos Aires, Buenos Aires, Argentina*
[4]*Piri Reis University, 34940 Tuzla, Istanbul, Turkey*
(Received 9 June 2011; published 5 October 2011)

We study the ground-state configurations of few interacting bosons confined in two dimensions by anisotropic harmonic potentials. By means of variational calculations, including correlation effects, we show that the arrangement of bosons strongly depends on the strength of the repulsive interaction and the anisotropy of the confinement. We compute the condensate fraction of the system and found that by increasing the anisotropy of the potential a weaker interaction suffices to destroy the condensate and favors the emergence of a crystal-like structure.

DOI: 10.1103/PhysRevA.84.043604 PACS number(s): 03.75.Lm, 03.75.Hh, 31.15.−p

I. INTRODUCTION

The interest in two-dimensional (2D) ensembles of a few bosons has increased in recent years due to the experimental achievements in the field of cold atoms (for a general review on cold atoms, see, e.g., Ref. [1]). In particular, the 2D distribution of line vortices has been extensively studied by a variety of experimental techniques [2,3] in atomic Bose-Einstein condensates (BEC) confined inside harmonic traps. A vortex created at the center of a stationary trap corresponds to a maximum of the energy functional and will tend to spiral out of the trap in a finite time [4], but the vortex state can be stabilized by setting the trap into rotation. On stirring the condensate at increasing frequency, first, one vortex and then several vortices are observed to enter the condensate, and such vortex assemblies ultimately form an ordered pattern. These arrangements of vortex lines closely resemble a triangular crystallite almost up to the condensate boundary, even though the gas is subject to the external trapping potential and is, therefore, inhomogeneous. Long-range interactions have appeared more recently when dealing with polar ultracold molecules [5]. In this case the interparticle interaction is of the dipole-dipole type, which in addition to being long-range is anisotropic and, thus, can be repulsive or attractive depending on the relative orientation of the molecules. It is even possible to tune the shape of the interaction potential by dressing rotational excitations [6].

However, the interest in 2D fluids of bosons is not new. Indeed, it was greatly stimulated by the seminal work of Nelson and Seung [7], who showed that a fluid of flux lines in strongly type II superconducting materials can be mapped onto this model system in statistical mechanics. The interaction potential law is given by $V(r) = V_0 K_0(r/r_0)$, with V_0 a coupling-strength parameter and $K_0(x)$ a modified Bessel function behaving as $-\ln(x)$ at short distances. Following an early variational Monte Carlo study [8], the transition between an Abrikosov lattice and a homogeneous liquid of vortices was studied within this mapping by means of the dislocation mechanism of melting [9] and of the density functional theory of freezing [10]. A first-order transition from an Abrikosov lattice to a bosonic superfluid of entangled vortices has also been demonstrated by the path-integral Monte Carlo method [11].

In the present work we report theoretical calculations of the structures taken by arrangements of a low number of bosons. It has been demonstrated, by work both on strongly interacting electrons in 2D semiconductor quantum dots [12] and on strongly coupled bosons interacting by either a contact potential or the e^2/r Coulomb law inside 2D harmonic traps [13], that information on the structure of few-particle crystallites can be obtained directly from the one-body density by means of calculations based on the unrestricted Hartree-Fock (HF) method, which breaks the rotational symmetry imposed by the circular confinement. More generally, an approximate treatment of a strongly correlated many-body system can, in principle, lead to states with spontaneously broken rotational symmetry, as discussed for instance by Ring and Schuck [14] and by Reimann and Manninen [15].

We use in this work this most simple theoretical method to evaluate the structure of small clusters of bosons by means of self-consistent variational calculations on harmonically trapped bosons using a permanental wave function approximation and a Gaussian function basis set. We shall focus in K_0 interacting bosons confined by anisotropic harmonic potentials in 2D and analyze the disappearance of Bose-Einstein condensation as a result of interactions and the anisotropy.

The contents of the paper are briefly described as follows. In Sec. II we introduce the model Hamiltonian and the essential formalism for its solution within a self-consistent variational approximation, leading to numerical calculations of the bosons arrangements that are presented and discussed in Sec. III. Finally, in Sec. IV we summarize our main conclusions. We refer at this point to recent calculations on the structure and the spectrum of classical 2D clusters with a logarithmic interaction potential [16] and on ordered structures formed in rotating ultracold Bose gases [17], as introductory to a broader view of the field.

*capuzzi@df.uba.ar

II. FORMALISM

We consider a 2D system of N identical bosons described by the Hamiltonian

$$\hat{H} = \int d\mathbf{r}\, \psi^\dagger(\mathbf{r})\hat{H}_0\psi(\mathbf{r}) + \frac{1}{2}\int d\mathbf{r}d\mathbf{r}'\, \psi^\dagger(\mathbf{r})\psi^\dagger(\mathbf{r}')V(|\mathbf{r}-\mathbf{r}'|)\psi(\mathbf{r}')\psi(\mathbf{r}), \quad (1)$$

where $\psi(\mathbf{r})$ and $\psi^\dagger(\mathbf{r})$ are the field operators, $\hat{H}_0 = p^2/(2m) + m(\omega_x^2x^2 + \omega_y^2y^2)/2$ is the single-particle Hamiltonian with m the bosons mass, ω_x and ω_y are the angular trap frequencies, and $V(r)$ is the interparticle repulsive potential taken as $V(r) = V_0K_0(r/r_0)$ involving a coupling strength parameter V_0 and a length scale r_0. In our variational formulation we consider the N-body wave function ψ that is taken as the totally symmetric product of single-particles orbitals, i.e., the permanent

$$\psi(\mathbf{r}_1,\ldots,\mathbf{r}_N) = \frac{1}{N!}\sum_{p=1}^{N!}\phi_{p(1)}(\mathbf{r}_1)\phi_{p(2)}(\mathbf{r}_2)\ldots\phi_{p(N)}(\mathbf{r}_N), \quad (2)$$

where $\phi_i(\mathbf{r})$ are the single-particle orbitals and the sum runs over all permutations p of indices 1 to N. The energy can be thus written as

$$\begin{aligned} E &= \langle\psi|\hat{H}|\psi\rangle/\langle\psi|\psi\rangle \\ &= \frac{1}{N!}\sum_{p_1,p_2=1}^{N!}\left[\binom{N}{1}H_{0,p1(1)p2(1)}\prod_{i=2}^{N}S_{p1(i)p2(i)} + \binom{N}{2}V_{p1(1)p1(2)p2(1)p2(2)}\prod_{i=3}^{N}S_{p1(i)p2(i)}\right] \\ &\quad\times\left[\sum_{p_1=1}^{N!}\prod_{i=1}^{N}S_{p1(i)i}\right]^{-1}, \end{aligned} \quad (3)$$

where the matrix elements are given by

$$\begin{cases} H_{0,ij} = \int d\mathbf{r}\,\phi_i^*(\mathbf{r})\hat{H}_0\,\phi_j(\mathbf{r}) \\ V_{ijkl} = \int d\mathbf{r}d\mathbf{r}'\,\phi_i^*(\mathbf{r})\phi_j^*(\mathbf{r}')V(|\mathbf{r}-\mathbf{r}'|)\phi_k(\mathbf{r}')\phi_l(\mathbf{r}) \end{cases} \quad (4)$$

and the overlap matrix reads

$$S_{ij} = \int d\mathbf{r}\,\phi_i(\mathbf{r})^*\phi_j(\mathbf{r})\,. \quad (5)$$

The use of nonorthogonal orbitals in the context of the unrestricted Bose-HF theory was initiated by Romanovsky *et al.* [13] for a system of two-dimensional confined bosons interacting with a Coulomb potential and using a Gaussian function basis set. More recently, it was extended to 1D using an optimized basis set [18]. Application of nonorthogonal functions have also appeared in studies of the build up of the relative phase between two Bose-Einstein condensates [19] and of Efimov states in trapped many-boson systems [20].

In the case of orthonormal orbitals, i.e., when S_{ij} is the Kronecker δ, the energy takes the more familiar expression

$$E = \sum_{i=1}^{N}n_iH_{0,ii} + \frac{1}{2}\sum_{i,j}n_in_j(V_{ijij}+V_{ijji}) - \frac{1}{2}\sum_i n_i(n_i+1)V_{iiii}, \quad (6)$$

where $n_i \geqslant 1$ (0) for an occupied (unoccupied) orbital.

The energy E in Eq. (3) will be given below in units of $\hbar\omega_y$. Scaling of distances by the harmonic-oscillator length $\ell_0 = \sqrt{\hbar/(m\omega_y)}$ will also be used. As basis functions we use N anisotropic Gaussian wave functions

$$\phi_i(\mathbf{r}) = \frac{1}{\sqrt{\pi\sigma_{xi}\sigma_{yi}}}\,e^{-\left[\frac{(x-x_i)^2}{2\sigma_{xi}^2}+\frac{(y-y_i)^2}{2\sigma_{yi}^2}\right]}, \quad (7)$$

where the set $\{x_i, y_i, \sigma_{yi}, \sigma_{xi}\}$ with $i = 1$ to N are determined variationally from the minimization of the energy. The choice of this basis allows us to analytically calculate the one-body energy terms $H_{0,ij}$ and overlap matrices S_{ij}, whereas the interaction terms must be calculated numerically due to the form of the interaction potential. This choice will heavily impact on the numerical cost of the calculation as the matrix elements of interaction does not have a known analytic expression as function of the variational parameters. In practice, this will limit the number of atoms that can be treated in a reasonable time.

Within this approach we have access to an approximation of the full many-body wave function which in turn can be used to extract information on the emergence of a condensate. In particular, one can calculate the one-particle reduced density matrix (1-RDM) which defines the condensate fraction according to the Penrose-Onsager criterion [21]. The 1-RDM is defined as

$$\rho_1(\mathbf{r},\mathbf{r}') = N\int \psi^*(\mathbf{r},\mathbf{r}_2,\ldots,\mathbf{r}_N)\,\psi(\mathbf{r}',\mathbf{r}_2,\ldots,\mathbf{r}_N) \times d\mathbf{r}_2\ldots d\mathbf{r}_N \quad (8)$$

and, being Hermitian, it can be diagonalized as

$$\rho_1(\mathbf{r},\mathbf{r}') = \sum_l N_l\,\varphi_l^*(\mathbf{r})\varphi_l(\mathbf{r}'). \quad (9)$$

The wave functions $\varphi_l(\mathbf{r})$ are determined from the eigenvalue problem

$$\int \rho_1(\mathbf{r},\mathbf{r}')\,\varphi_l(\mathbf{r}')d\mathbf{r}' = N_l\,\varphi_l(\mathbf{r}) \quad (10)$$

where N_l are the populations guaranteed to be positive due to the positivity of ρ_1. Since the density is normalized to the number of particles N, it must be that $\sum_l N_l = N$. However, note that N_l need not be an integer number. Indeed, the fact that N_l is a noninteger indicates that the optimized state cannot be described by a single permanent of orthogonal orbitals and thus it must contain some correlation. A single value N_l of the order of the number of particles indicates the formation of BEC since it corresponds to a many-body state where most particles, namely N_l, share the same single-particle wave function. The

condensate fraction is thus defined as N_0/N, where N_0 is the largest N_l.

Furthermore, it is straightforward to compute the correlation factor $g(\mathbf{r})$ and the dynamic structure factor $S(\mathbf{k})$. Here, we focus on the ground-state configurations and the emergence of the condensate only.

III. RESULTS AND DISCUSSION

In our numerical calculations we consider a trap with $\omega_x = (1-\alpha)^{1/2}\omega_0$, $\omega_y = \omega_0$, and take $\omega_0 = 2\pi \times 100\,\mathrm{s}^{-1}$ and several values of α. Following our previous investigations we focus on values of r_0 in the range from 10 to 50 μm which is much larger than the size of the noninteracting condensate of about 3 μm. Therefore, the K_0 potential provides an approximate logarithmic repulsion among the particles.

A. Ground-state configurations

The minimization of the energy was carried out using the simplex method [22] starting from random initial positions of the Gaussian wave functions and small random deviations of their widths from the noninteracting case for a circular trap $\sigma_i = 1$. The procedure was performed until a convergence of the energy on 10^{-5} was achieved. The interaction terms were integrated on a mesh of 300×150 points in the (r,θ) space of the relative coordinates.

In Fig. 1 we show the energies of the ground-state configurations with $N = 3$ to 9 particles as functions of the strength of the interaction potential. The case with the larger r_0 illustrates the importance of the repulsive core of the potential. In particular, the larger core gives rise to extended regions of repulsions which thereby increases the fraction of interaction energy in the ground state. For comparison we have added the energies obtained with a contact interparticle interaction $V(r) = g\delta(r)$ with strength $g = V_0 r_0^2$, where we observe that the interaction energy remains well below the kinetic one. This behavior depends on the number of particles since, for macroscopic condensates with large number of particles, the interaction energy largely exceeds the kinetic energy.

The geometric distribution of the particles can be seen in Fig. 2 for $N = 6$ particles and the two values of r_0. For low repulsions, the bosons form a condensate sharing the same wave function whose width depends slightly on the number of particles. As the interaction exceeds a critical value it is energetically favorable to increase the trapping energy by moving apart the particles while reducing the interaction energy. As previously found on cluster with other type of interaction potential [13,23], we observe that on increasing the number of particles, the geometric distribution changes strongly by filling successive rings with particles. For the K_0 potential we have found that a transition to a second ring depends on the value of r_0, for low values r_0 the transition occurs for $N = 5$ instead of $N = 6$ as it occurs with the purely logarithmic interaction or the K_0 with large r_0. This is to be contrasted with the case of the long-range Coulomb potential of Ref. [13] where the transition is seen to occur at $N = 6$.

The density profiles depicted in Fig. 2 break the circular symmetry of the underlying Hamiltonian. In general,

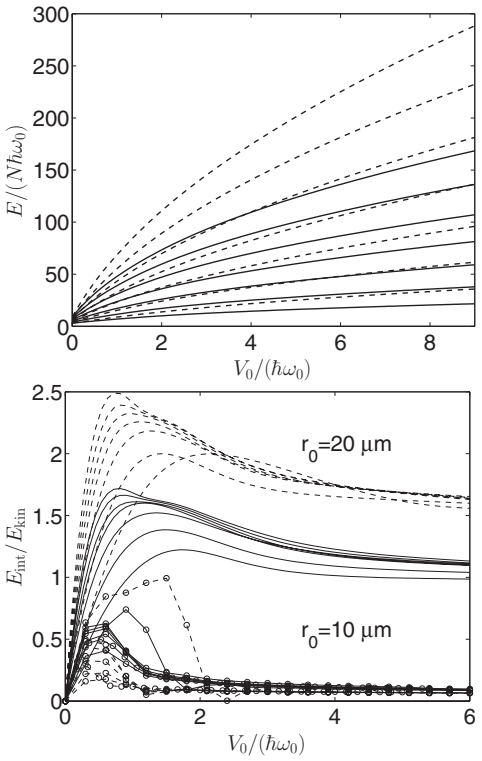

FIG. 1. Ground-state energies E (in units of $\hbar\omega_0$) for configurations with $N = 3$–9 particles in a circular trap as functions of the interaction V_0 (in units of $\hbar\omega_0$). The solid lines correspond to $r_0 = 10$ μm while the dashed ones to $r_0 = 20$ μm. (Top) Total energies, E; (bottom) ratio of the interaction ($E_{\rm int}$) to the kinetic ($E_{\rm kin}$) energy, where the lines with symbols correspond the the results obtained with the contact potentials of amplitude $V_0\, r_0^2$.

approximate treatments of correlated many-body problems can lead to states with spontaneously broken symmetries as studied, e.g., in the context of quantum dots in the self-consistent spin-and-space unrestricted HF treatment of the one-body density [15]. However, as any rotation of the broken symmetry state is a degenerate state, one can restore the circular symmetry by doing an appropriate superposition of rotated states. This symmetry restoration technique is widely known in nuclear physics [14] and has also been successfully demonstrated in applications to Wigner molecules

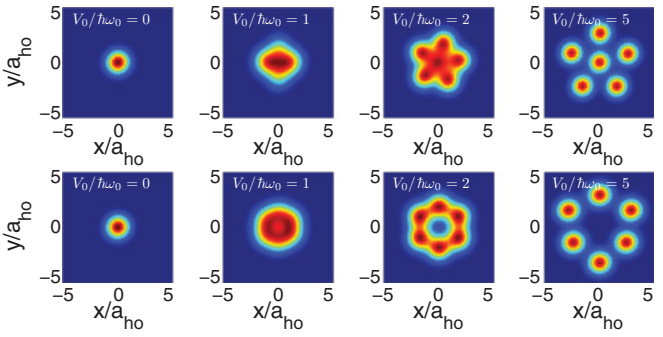

FIG. 2. (Color online) Ground-state density plots for $N = 6$ particles and several values of the interaction V_0 as indicated in the plot. The top and bottom rows correspond to $r_0 = 10$ μm and 50 μm, respectively.

of electrons in quantum dots [24] and in two-dimensional trapped bosons with $1/r$ interactions [13]. The technique provides a multipermanental (or determinantal in the case of electrons) state with the circular symmetry yielding a lower ground-state energy. Nevertheless, even in this case the underlying crystal-like structure can be revealed in the correlation factor $g(\mathbf{r},\mathbf{r}')$ containing information on the conditional probability of finding a particle at a given distance of another one [24,25].

While in macroscopic systems the emergence of spontaneously broken symmetry states is well known as, for instance, is the case of ferromagnetism. The case of finite systems is more subtle since quantum fluctuations cannot be usually neglected and one should apply more accurate techniques to have a definite answer on the nature of the ground state (for a review, see Ref. [26]). For electrons in 2D and for rotating condensates exact, diagonalization methods have confirmed that the ground state may possess a spontaneously broken symmetry depending on the strength of the interaction. However, here we are mainly interested in the effects of the noncircular trapping on the ground-state configurations where one only has discrete symmetries and hence we do not apply the restoration technique and defer the use of exact diagonalization techniques for future studies.

Next, we focus on the dependence of the geometric configurations on the anisotropy of the trap. The effects of the anisotropy can be summarized as follows: (i) for low V_0 the density profile follows the shape of the confinement as in a pure BEC, i.e., an anisotropic harmonic trap; (ii) for large V_0 the repulsive interaction breaks the condensate into a crystal-like structure and the anisotropy induces changes in the ordering of the atoms. For instance, for large V_0 and anisotropy we found that the distributions of atoms changes from a ring with an atom in its center [configuration (1,5)] to a distorted ring empty in its center [configuration (0,6)]. This change can be interpreted in terms of available space to accommodate the atoms in the trap as a function of the size of the repulsive core given by r_0. This effect is also observed for $N = 6$ and $N = 9$. The results for $N = 7$ and 8 are depicted in Figs. 3 and 4 for $r_0 = 10$ and 20 μm.

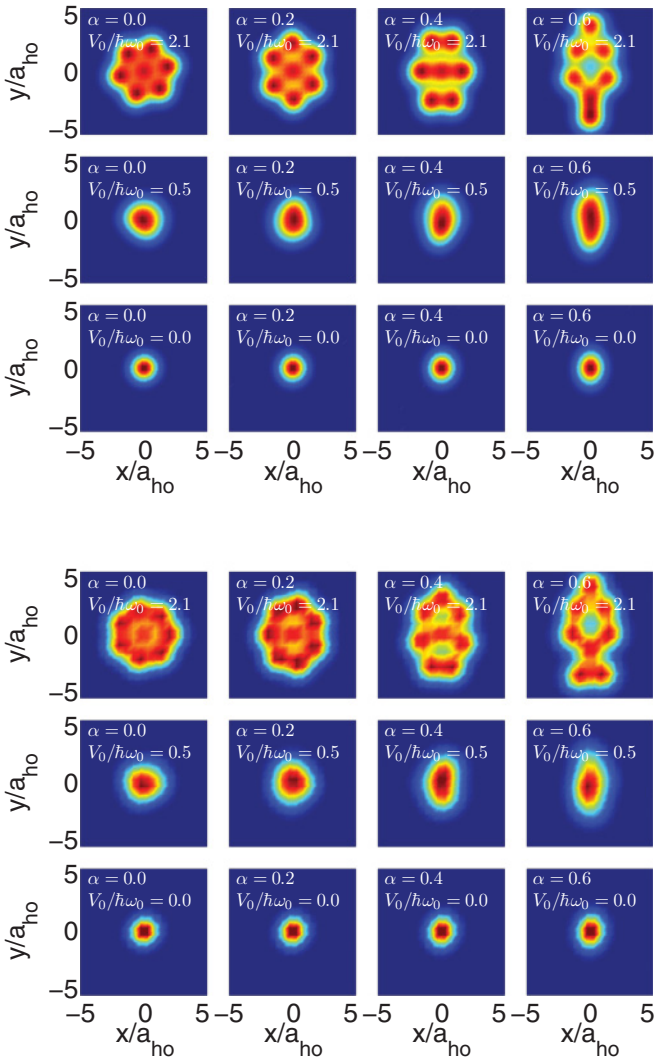

FIG. 3. (Color online) Density plots of configurations with $N = 7$ and $N = 8$ particles, and $r_0 = 10$ μm for several V_0 and α as indicated in the plot.

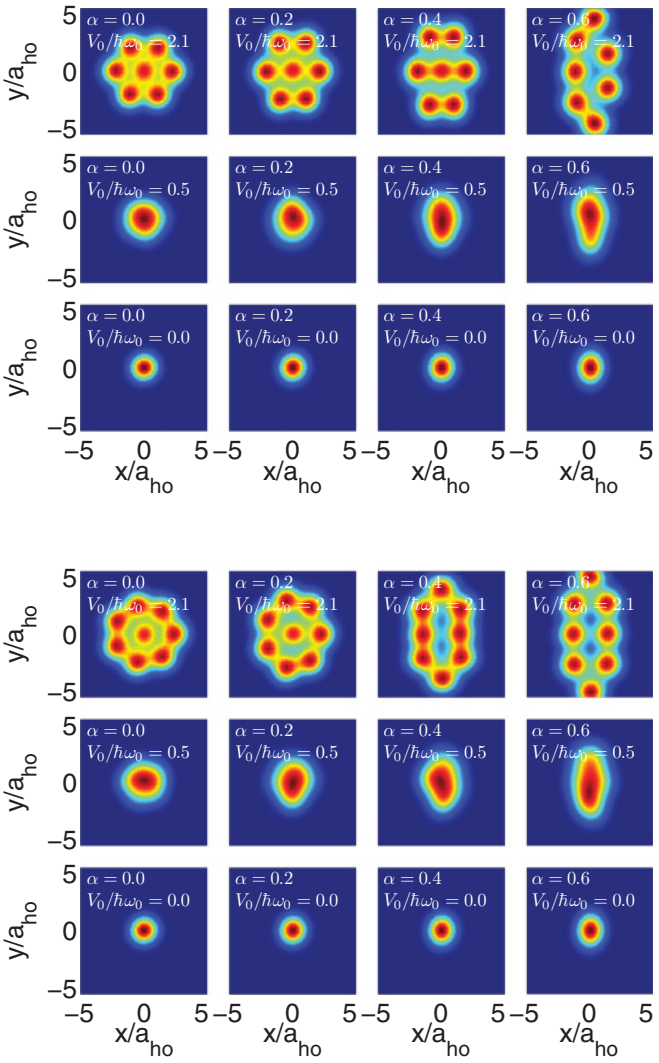

FIG. 4. (Color online) Density plots of configurations with $N = 7$ and $N = 8$ particles, and $r_0 = 20$ μm for several V_0 and α as indicated in the plot.

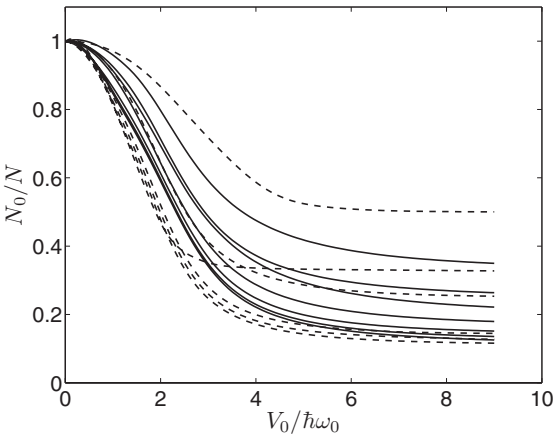

FIG. 5. Condensate fraction (N_0/N) as a function of V_0 (in units of $\hbar\omega_0$) for a circular trap with several values of N. The solid and dashed lines correspond to $r_0 = 10$ and 20 μm, respectively.

B. Condensate fraction

The calculation of the full wave function allowed us to estimate the condensate fraction. At large repulsions each atom occupies a single wave function forming a crystal-like structure and the condensate fraction is $1/N$; on the other hand, for vanishing interaction all atoms are Bose condensed into the same wave function and the condensate fraction equals 1. For increasing values of V_0, N_0 decreases and we observe that the transition toward the crystalline structure remains at about the same value $V_0 \simeq 4\hbar\omega_0$ irrespective of N. The results for the isotropic confinement are summarized in Fig. 5 for $N = 2$ to 9, while Fig. 6 shows the condensate wave function φ_0 for $N = 6$, $r_0 = 50$ μm and several values of V_0. The comparison with the total density in the bottom row of Fig. 2 illustrates how, for low V_0, the density profile is composed by an almost pure condensate, while for strong interactions each occupied orbital is located around a given density peak. We found that for $V_0/\hbar\omega_0 = 2$ there is still half the number of particles occupying the BEC phase while, at the same time, the appearance of a crystalline structure is clear.

The values of the condensate fraction in terms of V_0 and α enable us to construct a phase diagram with the Bose-condensed and non-Bose-condensed crystalline configurations. Even though the number of particles is very low and, therefore, the transition from the BEC phase to the noncondensed one is very broad, we can define the phase boundary as the critical interaction V_0^c where the function $N_0(V_0)$ changes the concavity sign for each value of α. In this manner, we obtain $V_0^c(\alpha)$, locating a rough border between the two phases. As a general trend we notice that for stronger anisotropy, larger α, and larger core sizes r_0, the

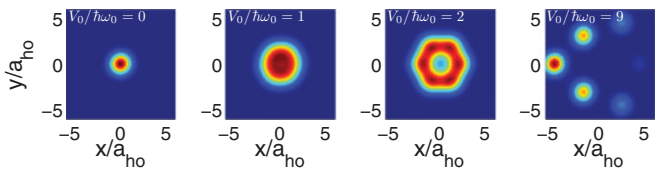

FIG. 6. (Color online) Density plots of φ_0 for $N = 6$ particles, $r_0 = 50$ μm and several V_0 as indicated in the plots.

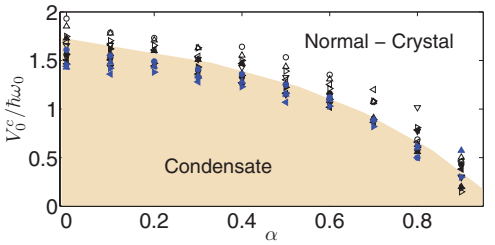

FIG. 7. (Color online) Critical interaction (in units of $\hbar\omega_0$) as a function of the anisotropy parameter α for several number of particles and core sizes. The open black and blue symbols correspond to $r_0 = 10$, 20, and 50 μm, respectively. The colored regions mark the two phases studied in the system.

phase boundary is shifted to lower interactions strengths. These results are summarized in Fig. 7.

IV. SUMMARY AND FINAL REMARKS

We studied the ground-state configurations of few bosons confined by a two-dimensional anisotropic harmonic potential and K_0 interaction potential relying on a minimal variational approach based in Gaussian wave functions. The approach incorporates the overlap among the basis wave functions and thus allow us to treat configurations spanning from Bose-Einstein condensates to crystal-like structures on the same footing. Additionally, this approach incorporates some correlation as the optimized many-body wave function cannot be written in term of a single permanent of orthogonal orbitals.

For isotropic confining potentials we found that, for the number of particles considered, the condensate fraction is seen to vanish at about the same magnitude of the interaction potential irrespective of the number of particles. In the case of the anisotropic trap, we found that by increasing the anisotropy parameter a smaller interaction drives the system out of the Bose-condensed phase.

Several improvements on the approach can be envisioned, for instance, the most straightforward would be to relax the Gaussian approximation of the wave functions, increase the number of basis functions above the number of particles, and/or, e.g., fully optimize the shape of the orbitals along the lines of what have been previously done for two bosons trapped in a symmetric double well [27]. These changes, however, would notably increase the computational demand. Another possible route to improve our treatment is to apply methods originally developed for quantum chemistry calculations as, for instance, the configuration interaction approximation. Some of these methods have been already extended to bosons in addition to atomic fermions [28,29].

ACKNOWLEDGMENTS

A.I.M. and S.E.O. acknowledge support from the Trakya University Research Fund under Projects No. TÜBAP-759 and TÜBAP-2008/42. P.C. acknowledges support from ANPCyT under PICT2008-0682, Argentina.

[1] G. Baym and C. J. Pethick, Phys. Rev. Lett. **76**, 6 (1996).
[2] M. R. Matthews, B. P. Anderson, P. C. Haljan, D. S. Hall, C. E. Wieman, and E. A. Cornell, Phys. Rev. Lett. **83**, 2498 (1999); K. W. Madison, F. Chevy, W. Wohlleben, and J. Dalibard, *ibid.* **84**, 806 (2000); J. R. Abo-Shaeer, C. Raman, J. M. Vogels, and W. Ketterle, Science **292**, 476 (2001); A. E. Leanhardt, A. Görlitz, A. P. Chikkatur, D. Kielpinski, Y. Shin, D. E. Pritchard, and W. Ketterle, Phys. Rev. Lett. **89**, 190403 (2002).
[3] A. L. Fetter and A. A. Svidzinsky, J. Phys. Condens. Matter **13**, R135 (2001).
[4] D. S. Rokhsar, Phys. Rev. Lett. **79**, 2164 (1997).
[5] J. Stuhler, A. Griesmaier, T. Koch, M. Fattori, T. Pfau, S. Giovanazzi, P. Pedri, and L. Santos, Phys. Rev. Lett. **95**, 150406 (2005).
[6] H. P. Büchler, E. Demler, M. Lukin, A. Micheli, N. Prokof'ev, G. Pupillo, and P. Zoller, Phys. Rev. Lett. **98**, 060404 (2007).
[7] D. R. Nelson and H. S. Seung, Phys. Rev. B **39**, 9153 (1989); see also P. Minnhagen, Rev. Mod. Phys. **59**, 1001 (1987).
[8] L. Xing and Z. Tesanovic, Phys. Rev. Lett. **65**, 794 (1990).
[9] H.-R. Ma and S. T. Chui, Phys. Rev. Lett. **67**, 505 (1991).
[10] S. Sengupta, C. Dasgupta, H. R. Krishnamurthy, G. I. Menon, and T. V. Ramakrishnan, Phys. Rev. Lett. **67**, 3444 (1991); G. I. Menon, C. Dasgupta, H. R. Krishnamurthy, T. V. Ramakrishnan, and S. Sengupta, Phys. Rev. B **54**, 16192 (1996).
[11] H. Nordborg and G. Blatter, Phys. Rev. Lett. **79**, 1925 (1997).
[12] C. Yannouleas and U. Landman, Phys. Rev. Lett. **82**, 5325 (1999); **85**, 2220 (2000); Phys. Rev. B **68**, 035325 (2003).
[13] I. Romanovsky, C. Yannouleas, and U. Landman, Phys. Rev. Lett. **93**, 230405 (2004).
[14] P. Ring and P. Schuck, *The Nuclear Many-Body Problem* (Springer, New York, 1980), p. 438ff.
[15] S. M. Reimann and M. Manninen, Rev. Mod. Phys. **74**, 1283 (2002).
[16] B. Partoens and P. S. Deo, Phys. Rev. B **69**, 245415 (2004); S. W. S. Apolinario, B. Partoens, and F. M. Peeters, Phys. Rev. E **72**, 046122 (2005).
[17] N. Barberán, M. Lewenstein, K. Osterloh, and D. Dagnino, Phys. Rev. A **73**, 063623 (2006).
[18] M. Heimsoth and M. Bonitz, Physica E **42**, 420 (2010).
[19] H. Xiong, S. Liu, and M. Zhan, New J. Phys. **8**, 245 (2006).
[20] D. V. Fedorov, A. S. Jensen, and M. Thgersen, Few-Body Syst. **43**, 69 (2008).
[21] O. Penrose and L. Onsager, Phys. Rev. **104**, 576 (1956).
[22] William H. Press, Saul A. Teukolsky, William T. Vetterling, and Brian P. Flannery, *Numerical Recipes: The Art of Scientific Computing*, 3rd ed. (Cambridge University Press, Cambridge, UK, 2007).
[23] M. Saint Jean and C. Guthmann, J. Phys.: Condens. Matter **14**, 13653 (2002).
[24] S. M. Reimann, M. Koskinen, and M. Manninen, Phys. Rev. B **62**, 8108 (2000).
[25] M. Gattobigio, P. Capuzzi, M. Polini, R. Asgari, and M. P. Tosi, Phys. Rev. B **72**, 045306 (2005).
[26] C. Yannouleas and U. Landman, Rep. Prog. Phys. **70**, 2067 (2007).
[27] A. I. Streltsov, O. E. Alon, and L. S. Cederbaum, Phys. Rev. A **73**, 063626 (2006).
[28] L. S. Cederbaum and A. I. Streltsov, Phys. Lett. A **318**, 564 (2003); Phys. Rev. A **70**, 023610 (2004); D. Masiello, S. B. McKagan, and W. P. Reinhardt, *ibid.* **72**, 063624 (2005).
[29] B. D. Esry, Phys. Rev. A **55**, 1147 (1997).